

# Beam Energy Dependence of the Third Harmonic of Azimuthal Correlations in Au+Au Collisions at RHIC

L. Adamczyk,<sup>1</sup> J. K. Adkins,<sup>20</sup> G. Agakishiev,<sup>18</sup> M. M. Aggarwal,<sup>31</sup> Z. Ahammed,<sup>49</sup> I. Alekseev,<sup>16</sup> A. Aparin,<sup>18</sup> D. Arkhipkin,<sup>3</sup> E. C. Aschenauer,<sup>3</sup> A. Attri,<sup>31</sup> G. S. Averichev,<sup>18</sup> X. Bai,<sup>7</sup> V. Bairathi,<sup>27</sup> R. Bellwied,<sup>45</sup> A. Bhasin,<sup>17</sup> A. K. Bhati,<sup>31</sup> P. Bhattarai,<sup>44</sup> J. Bielcik,<sup>10</sup> J. Bielcikova,<sup>11</sup> L. C. Bland,<sup>3</sup> I. G. Bordyuzhin,<sup>16</sup> J. Bouchet,<sup>19</sup> J. D. Brandenburg,<sup>37</sup> A. V. Brandin,<sup>26</sup> I. Bunzarov,<sup>18</sup> J. Butterworth,<sup>37</sup> H. Caines,<sup>53</sup> M. Calderón de la Barca Sánchez,<sup>5</sup> J. M. Campbell,<sup>29</sup> D. Cebra,<sup>5</sup> I. Chakaberia,<sup>3</sup> P. Chaloupka,<sup>10</sup> Z. Chang,<sup>43</sup> A. Chatterjee,<sup>49</sup> S. Chattopadhyay,<sup>49</sup> J. H. Chen,<sup>40</sup> X. Chen,<sup>22</sup> J. Cheng,<sup>46</sup> M. Cherney,<sup>9</sup> W. Christie,<sup>3</sup> G. Contin,<sup>23</sup> H. J. Crawford,<sup>4</sup> S. Das,<sup>13</sup> L. C. De Silva,<sup>9</sup> R. R. Debbe,<sup>3</sup> T. G. Dedovich,<sup>18</sup> J. Deng,<sup>39</sup> A. A. Derevschikov,<sup>33</sup> B. di Ruzza,<sup>3</sup> L. Didenko,<sup>3</sup> C. Dilks,<sup>32</sup> X. Dong,<sup>23</sup> J. L. Drachenberg,<sup>48</sup> J. E. Draper,<sup>5</sup> C. M. Du,<sup>22</sup> L. E. Dunkelberger,<sup>6</sup> J. C. Dunlop,<sup>3</sup> L. G. Efimov,<sup>18</sup> J. Engelage,<sup>4</sup> G. Eppley,<sup>37</sup> R. Esha,<sup>6</sup> O. Evdokimov,<sup>8</sup> O. Eyser,<sup>3</sup> R. Fatemi,<sup>20</sup> S. Fazio,<sup>3</sup> P. Federic,<sup>11</sup> J. Fedorisin,<sup>18</sup> Z. Feng,<sup>7</sup> P. Filip,<sup>18</sup> Y. Fisyak,<sup>3</sup> C. E. Flores,<sup>5</sup> L. Fulek,<sup>1</sup> C. A. Gagliardi,<sup>43</sup> D. Garand,<sup>34</sup> F. Geurts,<sup>37</sup> A. Gibson,<sup>48</sup> M. Girard,<sup>50</sup> L. Greiner,<sup>23</sup> D. Grosnick,<sup>48</sup> D. S. Gunarathne,<sup>42</sup> Y. Guo,<sup>38</sup> S. Gupta,<sup>17</sup> A. Gupta,<sup>17</sup> W. Guryn,<sup>3</sup> A. I. Hamad,<sup>19</sup> A. Hamed,<sup>43</sup> R. Haque,<sup>27</sup> J. W. Harris,<sup>53</sup> L. He,<sup>34</sup> S. Heppelmann,<sup>5</sup> S. Heppelmann,<sup>32</sup> A. Hirsch,<sup>34</sup> G. W. Hoffmann,<sup>44</sup> S. Horvat,<sup>53</sup> T. Huang,<sup>28</sup> X. Huang,<sup>46</sup> B. Huang,<sup>8</sup> H. Z. Huang,<sup>6</sup> P. Huck,<sup>7</sup> T. J. Humanic,<sup>29</sup> G. Igo,<sup>6</sup> W. W. Jacobs,<sup>15</sup> H. Jang,<sup>21</sup> A. Jentsch,<sup>44</sup> J. Jia,<sup>3</sup> K. Jiang,<sup>38</sup> E. G. Judd,<sup>4</sup> S. Kabana,<sup>19</sup> D. Kalinkin,<sup>15</sup> K. Kang,<sup>46</sup> K. Kauder,<sup>51</sup> H. W. Ke,<sup>3</sup> D. Keane,<sup>19</sup> A. Kechechyan,<sup>18</sup> Z. H. Khan,<sup>8</sup> D. P. Kikola,<sup>50</sup> I. Kisel,<sup>12</sup> A. Kisiel,<sup>50</sup> L. Kochenda,<sup>26</sup> D. D. Koetke,<sup>48</sup> L. K. Kosarzewski,<sup>50</sup> A. F. Kraishan,<sup>42</sup> P. Kravtsov,<sup>26</sup> K. Krueger,<sup>2</sup> L. Kumar,<sup>31</sup> M. A. C. Lamont,<sup>3</sup> J. M. Landgraf,<sup>3</sup> K. D. Landry,<sup>6</sup> J. Lauret,<sup>3</sup> A. Lebedev,<sup>3</sup> R. Lednicky,<sup>18</sup> J. H. Lee,<sup>3</sup> X. Li,<sup>42</sup> C. Li,<sup>38</sup> X. Li,<sup>38</sup> Y. Li,<sup>46</sup> W. Li,<sup>40</sup> T. Lin,<sup>15</sup> M. A. Lisa,<sup>29</sup> F. Liu,<sup>7</sup> T. Ljubicic,<sup>3</sup> W. J. Llope,<sup>51</sup> M. Lomnitz,<sup>19</sup> R. S. Longacre,<sup>3</sup> X. Luo,<sup>7</sup> R. Ma,<sup>3</sup> G. L. Ma,<sup>40</sup> Y. G. Ma,<sup>40</sup> L. Ma,<sup>40</sup> N. Magdy,<sup>41</sup> R. Majka,<sup>53</sup> A. Manion,<sup>23</sup> S. Margetis,<sup>19</sup> C. Markert,<sup>44</sup> H. S. Matis,<sup>23</sup> D. McDonald,<sup>45</sup> S. McKinzie,<sup>23</sup> K. Meehan,<sup>5</sup> J. C. Mei,<sup>39</sup> N. G. Minaev,<sup>33</sup> S. Mioduszewski,<sup>43</sup> D. Mishra,<sup>27</sup> B. Mohanty,<sup>27</sup> M. M. Mondal,<sup>43</sup> D. A. Morozov,<sup>33</sup> M. K. Mustafa,<sup>23</sup> B. K. Nandi,<sup>14</sup> Md. Nasim,<sup>6</sup> T. K. Nayak,<sup>49</sup> G. Nigmatkulov,<sup>26</sup> T. Niida,<sup>51</sup> L. V. Nogach,<sup>33</sup> S. Y. Noh,<sup>21</sup> J. Novak,<sup>25</sup> S. B. Nurushev,<sup>33</sup> G. Odyniec,<sup>23</sup> A. Ogawa,<sup>3</sup> K. Oh,<sup>35</sup> V. A. Okorokov,<sup>26</sup> D. Olvitt Jr.,<sup>42</sup> B. S. Page,<sup>3</sup> R. Pak,<sup>3</sup> Y. X. Pan,<sup>6</sup> Y. Pandit,<sup>8</sup> Y. Panebratsev,<sup>18</sup> B. Pawlik,<sup>30</sup> H. Pei,<sup>7</sup> C. Perkins,<sup>4</sup> P. Pile,<sup>3</sup> J. Pluta,<sup>50</sup> K. Poniatowska,<sup>50</sup> J. Porter,<sup>23</sup> M. Posik,<sup>42</sup> A. M. Poskanzer,<sup>23</sup> N. K. Pruthi,<sup>31</sup> J. Putschke,<sup>51</sup> H. Qiu,<sup>23</sup> A. Quintero,<sup>19</sup> S. Ramachandran,<sup>20</sup> S. Raniwala,<sup>36</sup> R. Raniwala,<sup>36</sup> R. L. Ray,<sup>44</sup> H. G. Ritter,<sup>23</sup> J. B. Roberts,<sup>37</sup> O. V. Rogachevskiy,<sup>18</sup> J. L. Romero,<sup>5</sup> L. Ruan,<sup>3</sup> J. Rusnak,<sup>11</sup> O. Rusnakova,<sup>10</sup> N. R. Sahoo,<sup>43</sup> P. K. Sahu,<sup>13</sup> I. Sakrejda,<sup>23</sup> S. Salur,<sup>23</sup> J. Sandweiss,<sup>53</sup> A. Sarkar,<sup>14</sup> J. Schambach,<sup>44</sup> R. P. Scharenberg,<sup>34</sup> A. M. Schmah,<sup>23</sup> W. B. Schmidke,<sup>3</sup> N. Schmitz,<sup>24</sup> J. Seger,<sup>9</sup> P. Seyboth,<sup>24</sup> N. Shah,<sup>40</sup> E. Shahaliev,<sup>18</sup> P. V. Shanmuganathan,<sup>19</sup> M. Shao,<sup>38</sup> A. Sharma,<sup>17</sup> B. Sharma,<sup>31</sup> M. K. Sharma,<sup>17</sup> W. Q. Shen,<sup>40</sup> Z. Shi,<sup>23</sup> S. S. Shi,<sup>7</sup> Q. Y. Shou,<sup>40</sup> E. P. Sichtermann,<sup>23</sup> R. Sikora,<sup>1</sup> M. Simko,<sup>11</sup> S. Singha,<sup>19</sup> M. J. Skoby,<sup>15</sup> N. Smirnov,<sup>53</sup> D. Smirnov,<sup>3</sup> W. Solyst,<sup>15</sup> L. Song,<sup>45</sup> P. Sorensen,<sup>3</sup> H. M. Spinka,<sup>2</sup> B. Srivastava,<sup>34</sup> T. D. S. Stanislaus,<sup>48</sup> M. Stepanov,<sup>34</sup> R. Stock,<sup>12</sup> M. Strikhanov,<sup>26</sup> B. Stringfellow,<sup>34</sup> M. Sumera,<sup>11</sup> B. Summa,<sup>32</sup> Z. Sun,<sup>22</sup> X. M. Sun,<sup>7</sup> Y. Sun,<sup>38</sup> B. Surrow,<sup>42</sup> D. N. Svirida,<sup>16</sup> Z. Tang,<sup>38</sup> A. H. Tang,<sup>3</sup> T. Tarnowsky,<sup>25</sup> A. Tawfik,<sup>52</sup> J. Thäder,<sup>23</sup> J. H. Thomas,<sup>23</sup> A. R. Timmins,<sup>45</sup> D. Tlusty,<sup>37</sup> T. Todoroki,<sup>3</sup> M. Tokarev,<sup>18</sup> S. Trentalange,<sup>6</sup> R. E. Tribble,<sup>43</sup> P. Tribedy,<sup>3</sup> S. K. Tripathy,<sup>13</sup> O. D. Tsai,<sup>6</sup> T. Ullrich,<sup>3</sup> D. G. Underwood,<sup>2</sup> I. Upsal,<sup>29</sup> G. Van Buren,<sup>3</sup> G. van Nieuwenhuizen,<sup>3</sup> M. Vandenbroucke,<sup>42</sup> R. Varma,<sup>14</sup> A. N. Vasiliev,<sup>33</sup> R. Vertesi,<sup>11</sup> F. Videbæk,<sup>3</sup> S. Vokal,<sup>18</sup> S. A. Voloshin,<sup>51</sup> A. Vossen,<sup>15</sup> F. Wang,<sup>34</sup> G. Wang,<sup>6</sup> J. S. Wang,<sup>22</sup> H. Wang,<sup>3</sup> Y. Wang,<sup>7</sup> Y. Wang,<sup>46</sup> G. Webb,<sup>3</sup> J. C. Webb,<sup>3</sup> L. Wen,<sup>6</sup> G. D. Westfall,<sup>25</sup> H. Wieman,<sup>23</sup> S. W. Wissink,<sup>15</sup> R. Witt,<sup>47</sup> Y. Wu,<sup>19</sup> Z. G. Xiao,<sup>46</sup> W. Xie,<sup>34</sup> G. Xie,<sup>38</sup> K. Xin,<sup>37</sup> Y. F. Xu,<sup>40</sup> Q. H. Xu,<sup>39</sup> N. Xu,<sup>23</sup> H. Xu,<sup>22</sup> Z. Xu,<sup>3</sup> J. Xu,<sup>7</sup> S. Yang,<sup>38</sup> Y. Yang,<sup>28</sup> Y. Yang,<sup>7</sup> C. Yang,<sup>38</sup> Y. Yang,<sup>22</sup> Q. Yang,<sup>38</sup> Z. Ye,<sup>8</sup> Z. Ye,<sup>8</sup> P. Yepes,<sup>37</sup> L. Yi,<sup>53</sup> K. Yip,<sup>3</sup> I. -K. Yoo,<sup>35</sup> N. Yu,<sup>7</sup> H. Zbroszczyk,<sup>50</sup> W. Zha,<sup>38</sup> X. P. Zhang,<sup>46</sup> Y. Zhang,<sup>38</sup> J. Zhang,<sup>39</sup> J. Zhang,<sup>22</sup> S. Zhang,<sup>40</sup> S. Zhang,<sup>38</sup> Z. Zhang,<sup>40</sup> J. B. Zhang,<sup>7</sup> J. Zhao,<sup>34</sup> C. Zhong,<sup>40</sup> L. Zhou,<sup>38</sup> X. Zhu,<sup>46</sup> Y. Zoukarneeva,<sup>18</sup> and M. Zyzak<sup>12</sup>

(STAR Collaboration)

<sup>1</sup>AGH University of Science and Technology, FPACS, Cracow 30-059, Poland

<sup>2</sup>Argonne National Laboratory, Argonne, Illinois 60439

<sup>3</sup>Brookhaven National Laboratory, Upton, New York 11973

<sup>4</sup>University of California, Berkeley, California 94720

- <sup>5</sup> *University of California, Davis, California 95616*  
<sup>6</sup> *University of California, Los Angeles, California 90095*  
<sup>7</sup> *Central China Normal University, Wuhan, Hubei 430079*  
<sup>8</sup> *University of Illinois at Chicago, Chicago, Illinois 60607*  
<sup>9</sup> *Creighton University, Omaha, Nebraska 68178*  
<sup>10</sup> *Czech Technical University in Prague, FNSPE, Prague, 115 19, Czech Republic*  
<sup>11</sup> *Nuclear Physics Institute AS CR, 250 68 Prague, Czech Republic*  
<sup>12</sup> *Frankfurt Institute for Advanced Studies FIAS, Frankfurt 60438, Germany*  
<sup>13</sup> *Institute of Physics, Bhubaneswar 751005, India*  
<sup>14</sup> *Indian Institute of Technology, Mumbai 400076, India*  
<sup>15</sup> *Indiana University, Bloomington, Indiana 47408*  
<sup>16</sup> *Alikhanov Institute for Theoretical and Experimental Physics, Moscow 117218, Russia*  
<sup>17</sup> *University of Jammu, Jammu 180001, India*  
<sup>18</sup> *Joint Institute for Nuclear Research, Dubna, 141 980, Russia*  
<sup>19</sup> *Kent State University, Kent, Ohio 44242*  
<sup>20</sup> *University of Kentucky, Lexington, Kentucky, 40506-0055*  
<sup>21</sup> *Korea Institute of Science and Technology Information, Daejeon 305-701, Korea*  
<sup>22</sup> *Institute of Modern Physics, Chinese Academy of Sciences, Lanzhou, Gansu 730000*  
<sup>23</sup> *Lawrence Berkeley National Laboratory, Berkeley, California 94720*  
<sup>24</sup> *Max-Planck-Institut für Physik, Munich 80805, Germany*  
<sup>25</sup> *Michigan State University, East Lansing, Michigan 48824*  
<sup>26</sup> *National Research Nuclear University MEPhI, Moscow 115409, Russia*  
<sup>27</sup> *National Institute of Science Education and Research, Bhubaneswar 751005, India*  
<sup>28</sup> *National Cheng Kung University, Tainan 70101*  
<sup>29</sup> *Ohio State University, Columbus, Ohio 43210*  
<sup>30</sup> *Institute of Nuclear Physics PAN, Cracow 31-342, Poland*  
<sup>31</sup> *Panjab University, Chandigarh 160014, India*  
<sup>32</sup> *Pennsylvania State University, University Park, Pennsylvania 16802*  
<sup>33</sup> *Institute of High Energy Physics, Protvino 142281, Russia*  
<sup>34</sup> *Purdue University, West Lafayette, Indiana 47907*  
<sup>35</sup> *Pusan National University, Pusan 46241, Korea*  
<sup>36</sup> *University of Rajasthan, Jaipur 302004, India*  
<sup>37</sup> *Rice University, Houston, Texas 77251*  
<sup>38</sup> *University of Science and Technology of China, Hefei, Anhui 230026*  
<sup>39</sup> *Shandong University, Jinan, Shandong 250100*  
<sup>40</sup> *Shanghai Institute of Applied Physics, Chinese Academy of Sciences, Shanghai 201800*  
<sup>41</sup> *State University Of New York, Stony Brook, NY 11794*  
<sup>42</sup> *Temple University, Philadelphia, Pennsylvania 19122*  
<sup>43</sup> *Texas A&M University, College Station, Texas 77843*  
<sup>44</sup> *University of Texas, Austin, Texas 78712*  
<sup>45</sup> *University of Houston, Houston, Texas 77204*  
<sup>46</sup> *Tsinghua University, Beijing 100084*  
<sup>47</sup> *United States Naval Academy, Annapolis, Maryland, 21402*  
<sup>48</sup> *Valparaiso University, Valparaiso, Indiana 46383*  
<sup>49</sup> *Variable Energy Cyclotron Centre, Kolkata 700064, India*  
<sup>50</sup> *Warsaw University of Technology, Warsaw 00-661, Poland*  
<sup>51</sup> *Wayne State University, Detroit, Michigan 48201*  
<sup>52</sup> *World Laboratory for Cosmology and Particle Physics (WLCAPP), Cairo 11571, Egypt*  
<sup>53</sup> *Yale University, New Haven, Connecticut 06520*

We present results from a harmonic decomposition of two-particle azimuthal correlations measured with the STAR detector in Au+Au collisions for energies ranging from  $\sqrt{s_{\text{NN}}} = 7.7$  GeV to 200 GeV. The third harmonic  $v_3^2\{2\} = \langle \cos 3(\phi_1 - \phi_2) \rangle$ , where  $\phi_1 - \phi_2$  is the angular difference in azimuth, is studied as a function of the pseudorapidity difference between particle pairs  $\Delta\eta = \eta_1 - \eta_2$ . Non-zero  $v_3^2\{2\}$  is directly related to the previously observed large- $\Delta\eta$  narrow- $\Delta\phi$  ridge correlations and has been shown in models to be sensitive to the existence of a low viscosity Quark Gluon Plasma (QGP) phase. For sufficiently central collisions,  $v_3^2\{2\}$  persist down to an energy of 7.7 GeV suggesting that QGP may be created even in these low energy collisions. In peripheral collisions at these low energies however,  $v_3^2\{2\}$  is consistent with zero. When scaled by pseudorapidity density of charged particle multiplicity per participating nucleon pair,  $v_3^2\{2\}$  for central collisions shows a minimum near  $\sqrt{s_{\text{NN}}} = 20$  GeV.

Researchers collide heavy nuclei at ultra-relativistic energies to create nuclear matter hot enough to form

a Quark Gluon Plasma (QGP) [1–4]; QGP permeated the entire universe in the first few microseconds after the Big Bang. Lattice QCD calculations show that the transition between hadronic matter and a QGP at zero baryon chemical potential is a smooth cross-over [5]. Data from the Relativistic Heavy Ion Collider (RHIC) at Brookhaven National Laboratory and at the Large Hadron Collider (LHC) at CERN have been argued to show that the matter created in these collisions is a nearly perfect fluid with a viscosity-to-entropy density ratio smaller than any other fluid known in nature [6–10]. At the higher collision energies, baryon number is not as easily transported from beam rapidity to mid-rapidity leaving the matter at mid-rapidity nearly net baryon free [11]. As  $\sqrt{s_{NN}}$  is decreased however, more baryon number can be transported to mid-rapidity creating a system with a larger net baryon density and larger baryon chemical potential ( $\mu_B$ ) [12–14]. Collisions with higher  $\mu_B$  values probe a region of the temperature- $\mu_B$  phase diagram, where the transition between QGP and hadrons may change from a smooth cross-over to a first-order phase transition [15], thus defining a possible critical point. In addition to having a larger  $\mu_B$ , collisions at lower  $\sqrt{s_{NN}}$  will also start with lower initial temperatures. For this reason, the system will spend relatively more time in the transition region until, at low enough  $\sqrt{s_{NN}}$ , it will presumably fail to create a QGP. It is not currently known at what  $\mu_B$  the transition might become first-order or at what  $\sqrt{s_{NN}}$  the collision region will become too cold to create a QGP. In this letter, we report on measurements of particle correlations that are expected to be sensitive to whether a low viscosity QGP phase has been created.

Correlations between particles emitted from heavy-ion collisions are particularly rich in information about the dynamics of the collision. It has been found that pairs of particles are preferentially emitted with small relative azimuthal angles ( $\Delta\phi = \phi_1 - \phi_2 \sim 0$ ) [16]. Surprisingly, this preference persists even when the particles are separated by large pseudo-rapidity ( $\eta$ ) gaps ( $\Delta\eta \gg 0$ ). These long-range correlations, known as the ridge, have been traced to the conversion of density anisotropies in the initial overlap of the two nuclei into momentum space correlations through subsequent interactions in the expansion [17–21]. Hydrodynamic models have been shown to require a low viscosity plasma phase early in the evolution to propagate the geometry fluctuations through pressure gradients into correlations between particles produced at freeze-out [7, 8]. Reduction in the pressure, as expected during a mixed phase for example, should lead to a reduction in the observed correlations [22–25]. The strength of correlations at different length scales can be studied through the analysis of  $v_n^2\{2\} = \langle \cos n(\Delta\phi) \rangle$  as a function of  $\Delta\eta$ . The second harmonic in this decomposition is dominated by asymmetries related to the elliptic shape of the collision overlap

region and has been studied for decades [26, 27]. The higher harmonics in this decomposition received attention more recently [16, 28–30] after the importance of the initial density fluctuations was realized [17–21]. The harmonic  $v_3^2\{2\}$  is thought to be particularly sensitive to the presence of a QGP phase: Hybrid model calculations show that while the large elliptic shape of the overlap region can develop into  $v_2^2\{2\}$  throughout the evolution, including the hadronic phase, the development of  $v_3^2\{2\}$  relies more strongly on the presence of a low viscosity QGP phase early in the collision [31, 32]. This suggests unless an alternative explanation for  $v_3^2\{2\}$  is found [33],  $v_3^2\{2\}$  will be an ideal observable to probe the formation of a QGP and the pressure gradients in the early plasma phase. In this letter we present measurements of  $v_3^2\{2\}(\Delta\eta)$  as a function of centrality in Au+Au collisions at  $\sqrt{s_{NN}} = 7.7, 11.5, 14.5, 19.6, 27, 39, 62.4$  and 200 GeV by the STAR detector at RHIC. We also compare these measurements to similar measurements from 2.76 TeV Pb+Pb collisions at the LHC [28].

The charged particles used in this analysis are detected through ionization energy loss in the STAR Time Projection Chamber [34]. The transverse momentum  $p_T$ ,  $\eta$ , and charge are determined from the trajectory of the track in the solenoidal magnetic field of the detector. With the 0.5 Tesla magnetic field used during data taking, particles can be reliably tracked for  $p_T > 0.2$  GeV/c. The efficiency for finding particles drops quickly as  $p_T$  decreases below this value [14]. Weights  $w_{i,j}$  have been used to correct the correlation functions for the  $p_T$ -dependent efficiency and for imperfections in the detector acceptance. The quantity analyzed and reported as  $v_n^2\{2\}(\Delta\eta)$  is

$$\langle \cos n(\Delta\phi) \rangle = \left\langle \left( \frac{\sum_{i,j,i \neq j} w_i w_j \cos n(\phi_i - \phi_j)}{\sum_{i,j,i \neq j} w_i w_j} \right) \right\rangle \quad (1)$$

where  $\sum_{i,j,i \neq j}$  is a sum over all unique pairs in an event and  $\langle \dots \rangle$  represents an average over events with each event weighted by the number of pairs in the event. The weights  $w_{i,j}$  are determined from the inverse of the  $\phi$  distributions after they have been averaged over many events (which for a perfect detector, should be flat) and by the  $p_T$  dependent efficiency. The  $w_{i,j}$  depend on the  $p_T$ ,  $\eta$ , and charge of the particle, the collision centrality, and the longitudinal position of the collision vertex. The correction procedure is verified by checking that the  $\phi$  distributions are flat after the correction and that  $\langle \cos n(\phi) \rangle$  and  $\langle \sin n(\phi) \rangle$  are much smaller than the  $\langle \cos(n\Delta\phi) \rangle$  [35]. With these corrections applied, the data represent the  $v_n^2\{2\}(\Delta\eta)$  that would be seen by a detector with perfect acceptance for particles with  $p_T > 0.2$  GeV/c and  $|\eta| < 1$ . Some previous results [30] on the  $\Delta\eta$  dependence of  $v_3^2\{2\}$  use average rather than differential corrections leading to small differences in the  $\Delta\eta$  dependence between that work and this work. The difference is largest in central collisions at  $1.5 < \Delta\eta < 2$  where the

$v_3^2\{2\}(\Delta\eta)$  reported previously is smaller by about 25%. The difference becomes less significant elsewhere. The data have been divided into standard centrality classes based on the number of charged hadrons observed for a given event within the pseudo-rapidity region  $|\eta| < 0.5$ . In some figures, we report the centrality in terms of the number of participating nucleons ( $N_{\text{part}}$ ) estimated from Monte Carlo Glauber calculations [14, 36].

In Fig. 1, we show examples of the third harmonic of the two-particle azimuthal correlation functions as a function of  $\Delta\eta$  for three centrality intervals (0%–5%, 20%–30%, and 60%–70%) and four energies ( $\sqrt{s_{\text{NN}}} = 200, 27, 14.5, \text{ and } 7.7 \text{ GeV}$ ). The harmonic  $v_3^2\{2\}$  exhibits a narrow peak in  $\Delta\eta$  centered at zero. For the more central collisions, non-zero  $v_3^2\{2\}$  persist out to large values of  $\Delta\eta$ . The non-zero values of  $v_3^2\{2\}$  at larger  $\Delta\eta$  are the result of a long-range correlation phenomena called the ridge which was first discovered in 200 GeV collisions at RHIC [16]. In central collisions, we observe that this long-range structure persists down to 7.7 GeV, the lowest beam energies measured at RHIC. In peripheral collisions, quantum interference effects grow broader owing to the inverse relationship between the size of the system and the width of the induced correlations. In peripheral collisions at 200 GeV, we observe an additional residual  $v_3^2\{2\}$  that, while not as wide as the ridge in central collisions, is still too wide to be attributed to quantum interference. At the lower beam energies however, the only  $v_3^2\{2\}$  signal present is at small  $\Delta\eta$  and the ridge-like structure is absent. These data indicate that for more central collisions, the ridge first seen at 200 GeV persists down to the much lower energies probed in the RHIC beam energy scan. In the peripheral collisions however, the ridge is absent at the lowest energies. The figure also shows calculations from UrQMD [37], a hadronic cascade model with no QGP phase. Although UrQMD produces a significant  $v_2$  in quantitative agreement with measurements at  $\sqrt{s_{\text{NN}}} < 20 \text{ GeV}$  [38], the model produces no appreciable  $v_3$ . The long-range correlations seen in Fig. 1 are only consistent with this hadronic model for peripheral collisions at the lower energies.

Short range correlations can arise from several sources including the fragmentation of hard or semi-hard scattered partons (jets) [39], from resonances, from quantum interference (HBT) [40], and from coulomb interference. In central collisions, a narrow peak arising primarily from HBT is present that is easy to isolate from other correlations. In order to study the remaining, longer-range correlations of interest in this letter, we simultaneously fit that short range correlation with a narrow Gaussian peak and the remaining correlations with a wider Gaussian with a constant offset. The fitting functions are shown in the figures where the solid curves represent the correlations of interest and the dashed curves represent the totals. We then extract  $v_3^2\{2\}$  averaged over  $\Delta\eta$  by excluding the contribution parameterized by the narrow

short-range Gaussian and integrating over the remaining structure within  $|\Delta\eta| < 2$ :

$$\langle v_3^2\{2\} \rangle = \frac{\int (dN/d\Delta\eta)(v_3^2\{2\}(\Delta\eta) - \delta)d\Delta\eta}{\int (dN/d\Delta\eta)d\Delta\eta} \quad (2)$$

where  $dN/d\Delta\eta$  is the number of pairs in each  $\Delta\eta$  bin (which decreases approximately linearly with  $\Delta\eta$  to zero at the edge of the acceptance) and  $\delta$  is the contribution from the narrow Gaussian. This quantity is extracted using the same procedure for different centralities and different beam energies. Our analysis does not attempt to isolate correlations attributed to flow from those attributed to other sources like jets and resonance decays (flow vs. non-flow) [41, 42]. Those non-flow correlations typically decrease with increasing multiplicity, and thus are not the dominating contribution in central collisions. This is especially so for the cases where  $v_3^2\{2\}$  is present in central collisions but absent in peripheral.

In Fig. 2, we present  $v_3^2\{2\}$  for charged hadrons integrated over  $p_T > 0.2 \text{ GeV}/c$  and  $|\eta| < 1$ , multiplied by  $N_{\text{part}}$  and plotted vs.  $N_{\text{part}}$ . The figure shows data for eight  $\sqrt{s_{\text{NN}}}$  values ranging from 7.7 to 200 GeV and for nine different centrality intervals corresponding to 0-5, 5-10, 10-20, 20-30, 30-40, 40-50, 60-70, and 70-80% most central. The corresponding average  $N_{\text{part}}$  values are estimated to be 350.6, 298.6, 234.3, 167.6, 117.1, 78.3, 49.3, 28.2 and 15.7 [14].  $N_{\text{part}}$  only weakly depends on energy and we use the same  $N_{\text{part}}$  values for all energies even though centrality resolution changes with  $\sqrt{s_{\text{NN}}}$ . We plot  $N_{\text{part}}v_3^2\{2\}$  to cancel the approximate  $1/N_{\text{part}}$  decrease one expects for two-particle correlations or fluctuations as  $N_{\text{part}}$  increases. If a central collision was a trivial linear superposition of p+p collisions, then  $N_{\text{part}}v_3^2\{2\}$  would remain constant with centrality. The data deviate drastically from the trivial expectation. In peripheral collisions,  $N_{\text{part}}v_3^2\{2\}$  is close to zero, but then increases with centrality until it saturates at values close to  $N_{\text{part}}=300$  before exhibiting a systematic tendency to drop slightly in the most central bins. This drop in the most central bin is there for all except the lowest energies where error bars become somewhat larger and the centrality resolution becomes worse. This rise and then fall has been traced to the non-trivial evolution of the initial geometry of two overlapping nuclei [45]; when the collisions are off-axis, the effect of fluctuations in positions of nucleons in one nucleus are enhanced when they collide with the center of the other nucleus (increasing  $v_3^2\{2\}$ ). This effect subsides when the two nuclei collide nearly head-on. The increase of  $N_{\text{part}}v_3^2\{2\}$  is exhibited at all energies including 7.7 GeV. Several models suggest that the absence of a QGP should be accompanied by a significant decrease in  $v_3^2\{2\}$  [31, 32], but we do not see that decrease. We include a comparison of the AMPT (Default) hadronic model to the 7.7 GeV data [32]. The non-QGP model predicts a smaller  $v_3^2\{2\}$  value than the



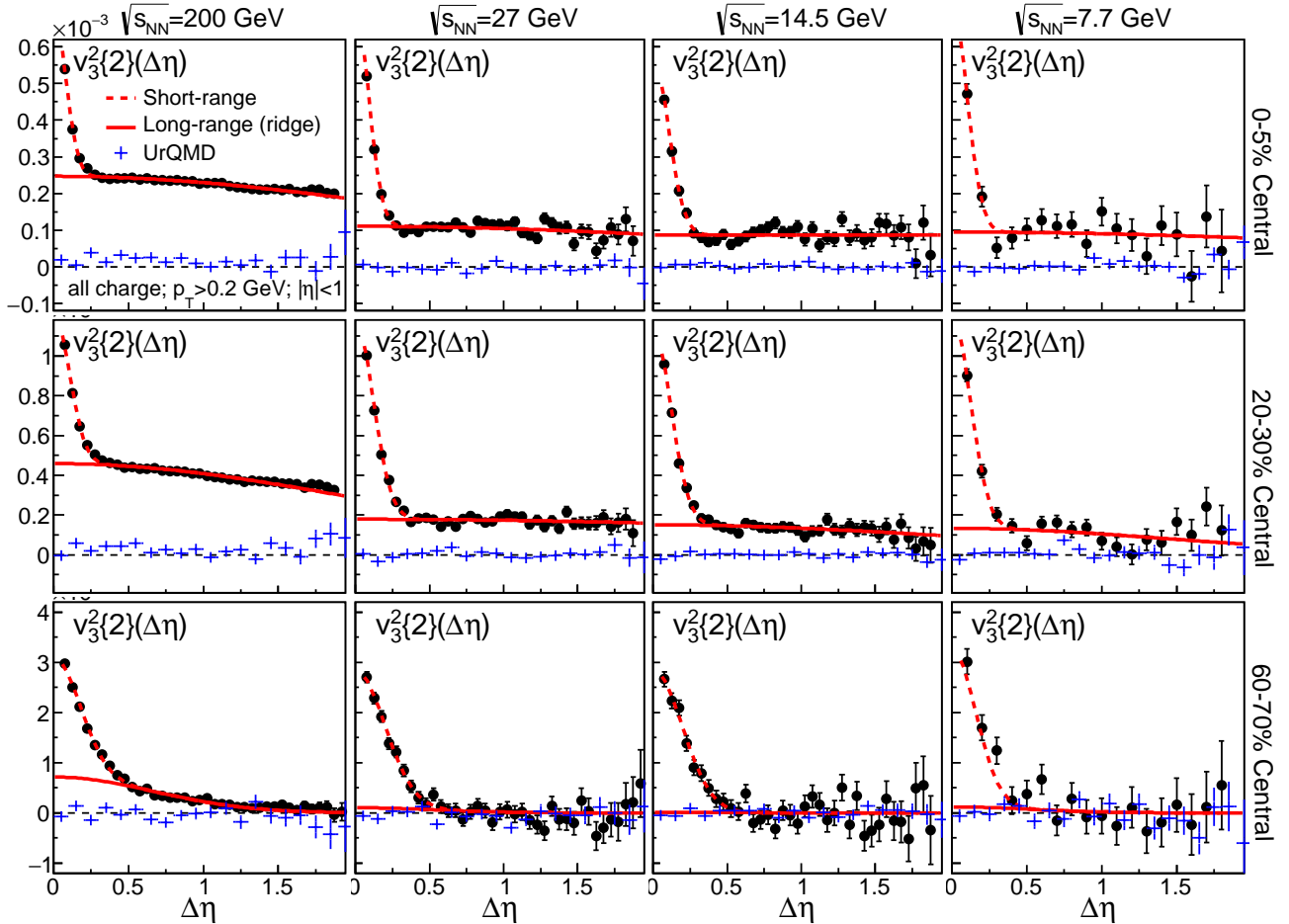


FIG. 1. (Color online) Representative results on  $v_3^2\{2\}$  from Au+Au collisions as a function of  $\Delta\eta$  for charged hadrons with  $p_T > 0.2$  GeV/c and  $|\eta| < 1$ . The columns (from left to right) show data from  $\sqrt{s_{NN}} = 200, 27, 14.5,$  and  $7.7$  GeV while the rows (from top to bottom) show data from 0%-5%, 20%-30%, and 60%-70% centrality intervals. The error bars show statistical uncertainties only. The fitted curves are described in the text. UrQMD [37] results are also shown.

data, suggesting that a QGP phase may exist in more central collisions at energies as low as 7.7 GeV.

Systematic errors on the integrated  $v_3^2\{2\}$  are studied by analyzing data from different years or from different periods of the run, by selecting events that collided at different z-vertex positions, by varying the efficiency correction within uncertainties, and by varying the selection criteria on tracks. A systematic uncertainty is also assigned based on the fitting and subtraction of the short range correlations (we assume a 10% uncertainty on the subtraction) and on residual acceptance corrections (10% of  $\langle \cos 3\phi \rangle^2 + \langle \sin 3\phi \rangle^2$ ). These errors are all added in quadrature for the final error estimate.

In Fig. 3, we re-plot the data from Fig. 2 for several centralities as a function of  $\sqrt{s_{NN}}$ . Data from 2.76 TeV Pb+Pb collisions are also included [28]. At 200 GeV, the 50%-60% central data are similar to the 30%-40% data. As the collision energy decreases however, values in

the peripheral 50%-60% centrality data group drop well below the 30%-40% central data and become consistent with zero for 7.7 and 11.5 GeV collisions. This shows again, that peripheral collisions at lower energies seem to fail to convert geometry fluctuations into a ridge-like correlation. This idea is consistent with the absence of a low viscosity QGP phase in low energy peripheral collisions [31]. For more central collisions however,  $v_3^2\{2\}$  is finite even at the lowest energies and changes very little from 7.7 GeV to 19.6 GeV. Above that, it begins to increase more quickly and roughly linearly with  $\log(\sqrt{s_{NN}})$ . This trend continues up to 2.76 TeV where for corresponding centrality intervals, the  $v_3^2\{2\}$  values are roughly twice as large as those at 200 GeV. Given that the dominant trend at the higher energies is for  $v_3^2\{2\}$  to increase with  $\log(\sqrt{s_{NN}})$ , it is notable that  $v_3^2\{2\}$  is approximately constant for the lower energies.

One would expect, independent of what energy range

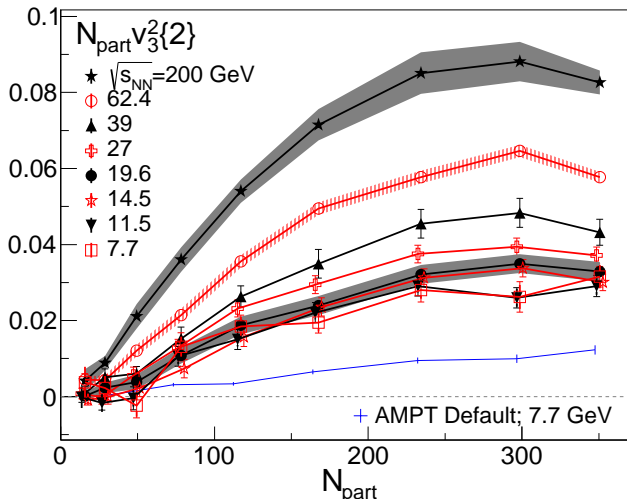


FIG. 2. The  $v_3^2\{2\}$  results from Au+Au collisions integrated over all  $\Delta\eta$  and multiplied by  $N_{\text{part}}$ . Statistical errors are typically smaller than the symbol size. Systematic errors are shown either as a shaded band or as thin vertical error bars with caps. The  $v_3^2\{2\}$  from a non-QGP based model, AMPT (Default), is also shown for  $\sqrt{s_{\text{NN}}}=7.7$  GeV for comparison [32].

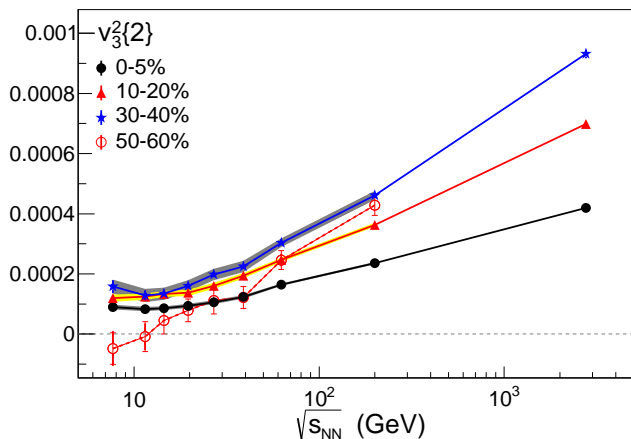


FIG. 3. The  $\sqrt{s_{\text{NN}}}$  dependence of  $v_3^2\{2\}$  for four representative centrality intervals. All data are Au+Au except for the 2.76 TeV data points from the ALICE collaboration [28] which are Pb+Pb. ALICE data are not available for the 50%-60% centrality interval.

is considered, that higher energy collisions producing more particles should be more effective at converting initial state geometry fluctuations into  $v_3^2\{2\}$ . Deviations from that expectation could indicate interesting physics like a softening of the equation-of-state [22]. We investigated these expectations at the lower  $\sqrt{s_{\text{NN}}}$  by scaling  $v_3^2\{2\}$  by the mid-rapidity, charged-particle multiplicity, pseudo-rapidity density per participant-pair

$$n_{\text{ch,PP}} = \frac{2}{N_{\text{part}}} dN_{\text{ch}}/d\eta.$$

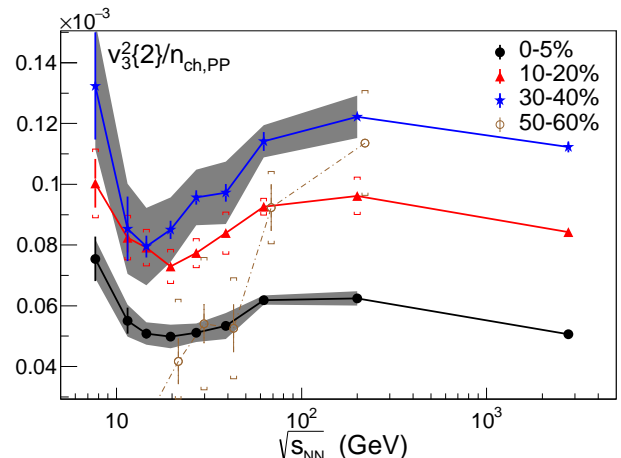


FIG. 4.  $v_3^2\{2\}$  divided by the mid-rapidity, charged particle multiplicity, pseudo-rapidity density per participant pair in Au+Au and Pb+Pb (2.76 TeV) collisions. Data in the centrality range from 0-50% exhibit a local minimum near 20 GeV while the more peripheral events do not.

We parameterize the  $\sqrt{s_{\text{NN}}}$  dependence of the existing data on  $n_{\text{ch,PP}}$  for central Au+Au or Pb+Pb collisions [46] by

$$n_{\text{ch,PP}} = \begin{cases} 0.77(\sqrt{s_{\text{NN}}})^{0.30} & \sqrt{s_{\text{NN}}} > 16.0 \text{ GeV} \\ 0.78 \log(\sqrt{s_{\text{NN}}}) - 0.4 & \text{otherwise} \end{cases} \quad (3)$$

In Fig. 4, we show  $v_3^2\{2\}/n_{\text{ch,PP}}$  for four centrality intervals. The more central data exhibit a local minimum in the  $\sqrt{s_{\text{NN}}}$  range around 15-20 GeV which is absent for peripheral collisions. Variations of  $v_3^2\{2\}/n_{\text{ch,PP}}$  with different parameterizations of  $n_{\text{ch,PP}}$  are typically on the order of a few percent. The trends in  $n_{\text{ch,PP}}$  also have a change in behavior in the same energy range where the dip appears in Fig. 4, but the apparent minima in the figure do not depend on the details of the parameterization of  $n_{\text{ch,PP}}$ ; the local minima remain even if scaling by  $\log(\sqrt{s_{\text{NN}}})$ . The minima are an inevitable consequence of the near independence of  $v_3^2\{2\}$  with respect to  $\sqrt{s_{\text{NN}}}$  for  $\sqrt{s_{\text{NN}}} < 20$  GeV while simultaneously, the multiplicity is monotonically increasing. If the otherwise general increase of  $v_3^2\{2\}$  is driven by ever increasing pressure gradients in ever denser systems at higher energies, then the local minimum in  $v_3^2\{2\}/n_{\text{ch,PP}}$  could be an indication of an anomalously low pressure inside the matter created in collisions with energies near 15-20 GeV. We note that the minima in Fig. 4 could depend on the specific scaling scheme and more rigorous theoretical modelling is needed to connect this measurement to the initial density and flow dynamics. In addition, the interpretation of data in this energy range is complicated by changes in the baryon to meson ratio [47], a relatively faster increase of  $\mu_B$  driven by baryon stopping [48], possible changes

in the sources and magnitude of non-flow [42], and the longer crossing times for nuclei at lower energies [31]. The existence of the minimum in  $v_3^2\{2\}/n_{\text{ch,PP}}$  and other provocative trends in data collected around these energies including the minimum in the slope of the net proton  $v_1$  [25] is interesting and provides ample motivation for further investigation [49].

In summary, we presented measurements of the  $\sqrt{s_{\text{NN}}}$  dependence of  $v_3^2\{2\}$  in Au+Au collisions for  $\sqrt{s_{\text{NN}}}$  energies ranging from 7.7 to 200 GeV. The conversion of density fluctuations in the initial-state have previously been found to provide a simple explanation for  $v_3^2\{2\}$  and the corresponding ridge correlations. Model calculations have shown that while  $v_2$  can also be established over a longer period in a higher viscosity hadronic phase,  $v_3^2\{2\}$  is particularly sensitive to the presence of a low viscosity plasma phase in the evolution of the collision. By studying the  $\Delta\eta$  dependence of  $v_3^2\{2\}$ , we find that for sufficiently central collisions ( $N_{\text{part}} > 50$ ), the ridge and  $v_3^2\{2\}$  persist down to the lowest energies studied. For more peripheral collisions however, the ridge correlation appears to be absent at low energies for  $N_{\text{part}} < 50$ , in agreement with certain non-QGP models. When comparing  $v_3^2\{2\}$  at RHIC and the LHC, the much larger multiplicities at the LHC lead to a much larger  $v_3^2\{2\}$ . When divided by multiplicity,  $v_3^2\{2\}$  shows a local minimum in the region near 15-20 GeV. This feature has not been shown in any known models of heavy ion collisions and could indicate an interesting trend in the pressure developed inside the system.

We thank the RHIC Operations Group and RCF at BNL, the NERSC Center at LBNL, the KISTI Center in Korea, and the Open Science Grid consortium for providing resources and support. This work was supported in part by the Office of Nuclear Physics within the U.S. DOE Office of Science, the U.S. NSF, the Ministry of Education and Science of the Russian Federation, NSFC, CAS, MoST and MoE of China, the National Research Foundation of Korea, NCKU (Taiwan), GA and MSMT of the Czech Republic, FIAS of Germany, DAE, DST, and UGC of India, the National Science Centre of Poland, National Research Foundation, the Ministry of Science, Education and Sports of the Republic of Croatia, and RosAtom of Russia.

---

[1] J. C. Collins and M. J. Perry, Phys. Rev. Lett. **34**, 1353 (1975).  
 [2] S. A. Chin, Phys. Lett. B **78**, 552 (1978).  
 [3] J. I. Kapusta, Nucl. Phys. B **148**, 461 (1979).  
 [4] R. Anishetty, P. Koehler and L. D. McLerran, Phys. Rev. D **22**, 2793 (1980).  
 [5] Y. Aoki, G. Endrodi, Z. Fodor, S. D. Katz and K. K. Szabo, Nature **443**, 675 (2006).  
 [6] I. Arsene *et al.* [BRAHMS Collaboration], Nucl. Phys.

A **757**, 1 (2005); B. B. Back *et al.* [PHOBOS Collaboration], Nucl. Phys. A **757**, 28 (2005); J. Adams *et al.* [STAR Collaboration], Nucl. Phys. A **757**, 102 (2005); K. Adcox *et al.* [PHENIX Collaboration], Nucl. Phys. A **757**, 184 (2005).  
 [7] B. Muller, Acta Phys. Polon. B **38**, 3705 (2007); W. A. Zajc, Nucl. Phys. A **805**, 283 (2008).  
 [8] C. Gale, S. Jeon, B. Schenke, P. Tribedy and R. Venugopalan, Phys. Rev. Lett. **110**, no. 1, 012302 (2013).  
 [9] S. Chatrchyan *et al.* [CMS Collaboration], Phys. Rev. C **89**, no. 4, 044906 (2014).  
 [10] B. B. Abelev *et al.* [ALICE Collaboration], JHEP **1506**, 190 (2015).  
 [11] C. Adler *et al.* [STAR Collaboration], Phys. Rev. Lett. **86**, 4778 (2001) [Phys. Rev. Lett. **90**, 119903 (2003)].  
 [12] H. Appelshauser *et al.* [NA49 Collaboration], Phys. Rev. Lett. **82**, 2471 (1999).  
 [13] J. Adams *et al.* [STAR Collaboration], Phys. Rev. Lett. **92**, 112301 (2004).  
 [14] B. I. Abelev *et al.* [STAR Collaboration], Phys. Rev. C **79**, 034909 (2009).  
 [15] F. R. Brown *et al.*, Phys. Rev. Lett. **65**, 2491 (1990); A. Mocsy, F. Sannino and K. Tuominen, Phys. Rev. Lett. **92**, 182302 (2004); F. Karsch and M. Lutgemeier, "Deconfinement and chiral symmetry restoration in an SU(3) gauge theory Nucl. Phys. B **550**, 449 (1999); A. Barducci, R. Casalbuoni, G. Pettini and R. Gatto, Phys. Rev. D **49**, 426 (1994); A. M. Halasz, A. D. Jackson, R. E. Shrock, M. A. Stephanov and J. J. M. Verbaarschot, Phys. Rev. D **58**, 096007 (1998); O. Scavenius, A. Mocsy, I. N. Mishustin and D. H. Rischke, Phys. Rev. C **64**, 045202 (2001); N. G. Antoniou and A. S. Kapoyannis, Phys. Lett. B **563**, 165 (2003); Y. Hatta and T. Ikeda, Phys. Rev. D **67**, 014028 (2003); M. A. Stephanov, K. Rajagopal and E. V. Shuryak, Phys. Rev. Lett. **81**, 4816 (1998).  
 [16] J. Adams *et al.* [STAR Collaboration], Phys. Rev. C **73**, 064907 (2006); J. Adams *et al.* [STAR Collaboration], Phys. Rev. C **75**, 034901 (2007); J. Adams *et al.* [STAR Collaboration], Phys. Rev. Lett. **95**, 152301 (2005); A. Adare *et al.* [PHENIX Collaboration], Phys. Rev. C **78** (2008) 014901; B. I. Abelev *et al.* [STAR Collaboration], Phys. Rev. C **80**, 064912 (2009); B. Alver *et al.* [PHOBOS Collaboration], Phys. Rev. Lett. **104**, 062301 (2010); B. I. Abelev *et al.* [STAR Collaboration], Phys. Rev. Lett. **105**, 022301 (2010); S. Chatrchyan *et al.* [CMS Collaboration], JHEP **1107**, 076 (2011); K. Aamodt *et al.* [ALICE Collaboration], Phys. Lett. B **708**, 249 (2012); G. Aad *et al.* [ATLAS Collaboration], Phys. Rev. C **86**, 014907 (2012).  
 [17] S. A. Voloshin, Nucl. Phys. A **749**, 287 (2005).  
 [18] A. P. Mishra, R. K. Mohapatra, P. S. Saumia, A. M. Srivastava, Phys. Rev. C **77**, 064902 (2008).  
 [19] P. Sorensen, [arXiv:0808.0503 [nucl-ex]]; P. Sorensen, J. Phys. G **37**, 094011 (2010).  
 [20] J. Takahashi *et al.*, Phys. Rev. Lett. **103**, 242301 (2009).  
 [21] B. Alver, G. Roland, Phys. Rev. C **81**, 054905 (2010).  
 [22] H. Sorge, Phys. Rev. Lett. **82**, 2048 (1999).  
 [23] S. A. Voloshin and A. M. Poskanzer, Phys. Lett. B **474**, 27 (2000).  
 [24] H. Stoecker, Nucl. Phys. A **750**, 121 (2005).  
 [25] L. Adamczyk *et al.* [STAR Collaboration], Phys. Rev. Lett. **112**, no. 16, 162301 (2014).  
 [26] K. H. Ackermann *et al.* [STAR Collaboration], Phys. Rev. Lett. **86**, 402 (2001); J. Adams *et al.* [STAR Collab-

- oration], Phys. Rev. Lett. **92**, 052302 (2004); J. Adams *et al.* [STAR Collaboration], Phys. Rev. C **72**, 014904 (2005).
- [27] S. A. Voloshin, A. M. Poskanzer, R. Snellings, in *Landolt-Boernstein, Relativistic Heavy Ion Physics* (Springer-Verlag, Berlin, 2010), Vol. **1/23**, p. 5. [arXiv:0809.2949 [nucl-ex]]; P. Sorensen, in *Quark-Gluon Plasma 4* (World Scientific, Singapore, 2010), p. 323 [arXiv:0905.0174 [nucl-ex]]; H. G. Ritter and R. Stock, J. Phys. G **41**, 124002 (2014).
- [28] K. Aamodt *et al.* [ALICE Collaboration], Phys. Rev. Lett. **107**, 032301 (2011).
- [29] A. Adare *et al.* [PHENIX Collaboration], Phys. Rev. Lett. **107**, 252301 (2011).
- [30] L. Adamczyk *et al.* [STAR Collaboration], Phys. Rev. C **88**, no. 1, 014904 (2013).
- [31] J. Auvinen and H. Petersen, Phys. Rev. C **88**, no. 6, 064908 (2013).
- [32] D. Solanki, P. Sorensen, S. Basu, R. Raniwala and T. K. Nayak, Phys. Lett. B **720**, 352 (2013).
- [33] L. He, T. Edmonds, Z. W. Lin, F. Liu, D. Molnar and F. Wang, arXiv:1502.05572 [nucl-th].
- [34] STAR Collaboration, C. Adler *et al.*, Nucl. Instr. Meth. A **499**, 624 (2003).
- [35] A. Bilandzic, R. Snellings and S. Voloshin, Phys. Rev. C **83**, 044913 (2011); A. Bilandzic, C. H. Christensen, K. Gulbrandsen, A. Hansen and Y. Zhou, Phys. Rev. C **89**, no. 6, 064904 (2014).
- [36] M. L. Miller, K. Reygers, S. J. Sanders and P. Steinberg, Ann. Rev. Nucl. Part. Sci. **57**, 205 (2007).
- [37] S. A. Bass *et al.*, Prog. Part. Nucl. Phys. **41**, 255 (1998).
- [38] H. Petersen, Q. Li, X. Zhu and M. Bleicher, Phys. Rev. C **74**, 064908 (2006).
- [39] J. Adams *et al.* [STAR Collaboration], Phys. Rev. Lett. **97**, 162301 (2006).
- [40] M. A. Lisa, S. Pratt, R. Soltz and U. Wiedemann, Ann. Rev. Nucl. Part. Sci. **55**, 357 (2005).
- [41] N. Borghini, P. M. Dinh and J. Y. Ollitrault, Phys. Rev. C **64**, 054901 (2001).
- [42] N. M. Abdelwahab *et al.* [STAR Collaboration], Phys. Lett. B **745**, 40 (2015).
- [43] J. Adams *et al.* [STAR Collaboration], J. Phys. G **32**, L37 (2006).
- [44] G. Agakishiev *et al.* [STAR Collaboration], Phys. Rev. C **86**, 064902 (2012).
- [45] P. Sorensen, B. Bolliet, A. Mocsy, Y. Pandit and N. Pruthi, Phys. Lett. B **705**, 71 (2011).
- [46] B. Alver *et al.* [PHOBOS Collaboration], Phys. Rev. C **83**, 024913 (2011); K. Aamodt *et al.* [ALICE Collaboration], Phys. Rev. Lett. **105**, 252301 (2010).
- [47] P. Braun-Munzinger, J. Cleymans, H. Oeschler and K. Redlich, Nucl. Phys. A **697**, 902 (2002).
- [48] I. C. Arsene *et al.* [BRAHMS Collaboration], Phys. Lett. B **677**, 267 (2009).
- [49] U. Heinz, P. Sorensen, A. Deshpande, C. Gagliardi, F. Karsch, T. Lappi, Z. E. Meziani and R. Milner *et al.*, arXiv:1501.06477 [nucl-th]; Y. Akiba, A. Angerami, H. Caines, A. Frawley, U. Heinz, B. Jacak, J. Jia and T. Lappi *et al.*, arXiv:1502.02730 [nucl-ex].